DALTON
FULL PAPER

Mononuclear and dinuclear ruthenium(II)/(III) salicylates incorporating azoimine functionalities as ancillary ligands. Synthesis, spectroscopic and electron-transfer properties †

Ramapati Samanta, Biplab Mondal, Pradip Munshi and Goutam Kumar Lahiri *

Department of Chemistry, Indian Institute of Technology, Bombay, Powai, Mumbai-400076, India

Received 3rd January 2001, Accepted 12th April 2001
First published as an Advance Article on the web 25th May 2001

Ruthenium–salicylate complexes incorporating azoimine based azopyridine ligands, L, of the type $[Ru^{II}(L)_2$-(salicylate)] **1**–**5** [L = $NC_5H_4N{=}NC_6H_4(R)$, R = H, *m*-Me/Cl or *p*-Me/Cl] have been synthesized and their spectroelectrochemical aspects investigated. The complexes systematically exhibit two $1e^-$ and two $2e^-$ oxidation processes and four successive one-electron reductions. The stepwise electrochemical oxidations were followed by electronic and EPR spectral studies on each oxidation step which indicate that the initial one-electron oxidation process corresponds to stereoretentive oxidation of the ruthenium(II) centre to ruthenium(III), $[Ru^{III}(L)_2$(salicylate)]$^+$ $\mathbf{1}^+$–$\mathbf{5}^+$. The second oxidation step corresponds to oxidation of the coordinated salicylate moiety in $\mathbf{1}^+$–$\mathbf{5}^+$ to the ruthenium(III)–salicylate semiquinone cationic radical, $[Ru^{III}(L)_2$(salicylate)]$^{2+}$ **E**. The electrogenerated ruthenium(III) congeners ($\mathbf{1}^+$–$\mathbf{5}^+$) exhibit rhombic EPR spectra corresponding to distorted octahedral complexes. The electrogenerated semiquinone salicylate radical $[Ru^{III}(L)_2$(salicylate)]$^{2+}$ **E** undergoes a radical recombination process which leads to formation of antiferromagnetically coupled dimeric species, $[(L)_2Ru^{III}(X)Ru^{III}(L)_2]^{4+}$ **F** [(X = $^-O_2C(O)$-$C_6H_4C_6H_4(O)CO_2^-$]. The next two $2e^-$ oxidation processes are associated with oxidation of the bridging moiety of the dimeric species $[(L)_2Ru^{III}(X')Ru^{III}(L)_2]^{4+}$ **G** [(X′ = $^-O_2C(O)C_6H_3{=}C_6H_3(O)CO_2^-$] followed by oxidation of the metal centres, $[(L)_2Ru^{IV}(X')Ru^{IV}(L)_2]^{6+}$ **H**. The chemical oxidation of the complexes **1**–**5** by HNO_3 leads to formation of dimeric complexes, **G**, straightaway. The complexes display intense charge-transfer bands in the UV-visible region which have been found to be reasonably blue shifted while moving from **1**–**5** to $\mathbf{1}^+$–$\mathbf{5}^+$ to **F** to **G**.

Introduction

The relevance of salicylic acid in a wide range of biological applications[1] besides its potential use as a chelating function[2] makes it a molecule of profound interest. Moreover, it has been observed recently that the salicylate function undergoes fascinating electron-transfer properties on coordination to the $Ru(bpy)_2$ core, $[Ru(bpy)_2$(salicylate)] **1** (bpy = 2,2′-bipyridine). This leads to hydroxylation of the electrogenerated coordinated salicylate semiquinone intermediate (**E**) *via* successive electron transfer processes.[3] The observed electro-non-innocent behaviour of the salicylate function on coordination to $Ru(bpy)_2$ has prompted us to examine its reactivity particularly in combination with bipyridine like, but stronger π-acidic arylazopyridine ligands L, $[Ru(L)_2$(salicylate)] [L = $NC_5H_4N{=}NC_6H_4(R)$, R = H, *m*-Me/Cl or *p*-Me/Cl]. The present study shows that in the presence of L the electrogenerated salicylate semiquinone radical (**E**) preferentially follows a radical recombination process leading to the formation of a dimeric species **F** as a reactive intermediate. This dimeric species is found to undergo further successive proton transfer and electron transfer processes.

Herein we report the synthesis and detailed spectroelectrochemical properties of the complexes $[Ru(L)_2$(salicylate)]

† Electronic supplementary information (ESI) available: electrospray mass spectra of complexes **1** and **1G**. See http://www.rsc.org/suppdata/dt/b1/b100163i/

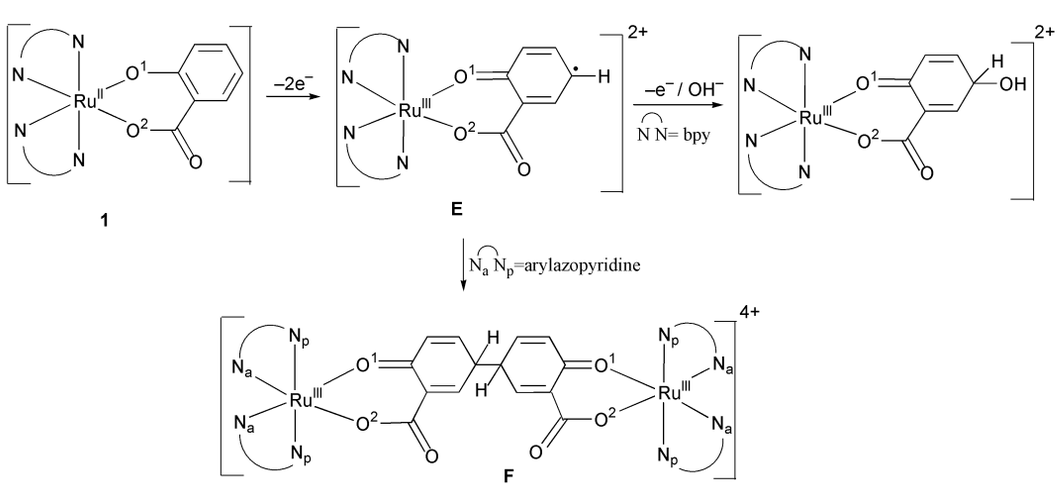

and monomer to dimer conversion as a function of electron-transfer processes at the salicylate moiety.

Results

Synthesis and characterisation

Ruthenium(II) salicylate complexes, $[Ru^{II}(L)_2(salicylate)]$ **1**–**5** [L = $NC_5H_4N{=}NC_6H_4(R)$, R = H, *m*-Me/Cl or *p*-Me/Cl] incorporating azoimine based azopyridine ($L^{1–5}$) ancillary ligands have been synthesized from the starting *ctc*-$Ru^{II}(L)_2Cl_2$ species (*ctc* = *cis*-*trans*-*cis* with respect to chlorides, pyridine and azo nitrogens respectively) (Scheme 1). The salicylate group binds to the ruthenium ion as the usual binegative function, resulting in neutral and diamagnetic ruthenium(II) heterochelates (**1**–**5**).

The microanalytical data of the complexes match well with the calculated values (Experimental section). The unsymmetric nature of L and the salicylate functions lead to the possibility of coexistence of four geometrical isomers (**A**–**D**). However, the

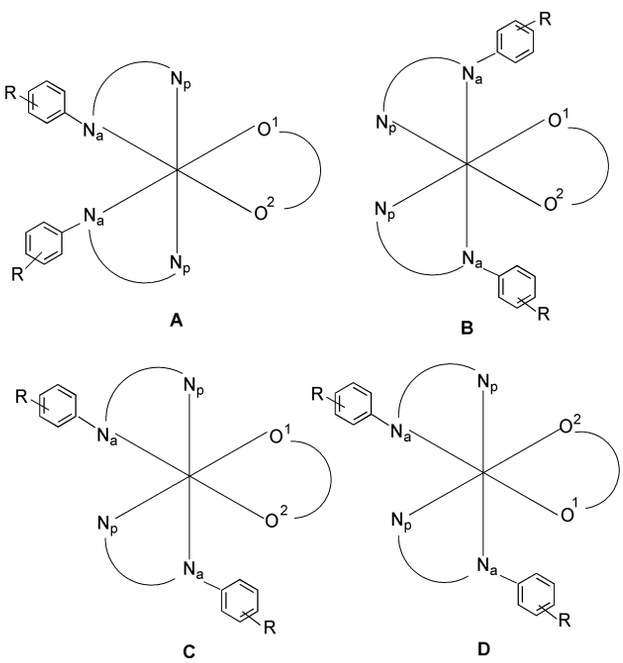

complexes (**1**–**5**) constantly develop into one particular blue-violet isomer. Since the *tc* (*trans* and *cis* with respect to pyridine and azo nitrogens respectively) configuration of the starting $Ru(L)_2$ fragment is known thermodynamically to be most stable and has been observed to retain the *tc* identity in all other reported complexes incorporating the $Ru(L)_2$ moiety,[4] it may be assumed that the reactions in Scheme 1 also follow the stereo-retentive pathway (structure **A**).

The oxidation of the complexes **1**–**5** by using concentrated HNO_3 results in a stable red dimeric product (**G**, Scheme 2). Although all the complexes (**1**–**5**) behave similarly on HNO_3 oxidation; the oxidised complex $[(L^1)_2Ru^{III}\{^{-}O_2C(O)C_6H_3{=}C_6H_3(O)CO_2^{-}\}Ru^{III}(L^1)_2][ClO_4]_4{\cdot}2H_2O$ **1G** has been isolated in the solid state as its dihydrated perchlorate salt. It may be noted that HNO_3 was also used earlier for the selective oxidation of $[Ru^{II}(L)_2Cl_2] \longrightarrow [Ru^{III}(L)_2Cl_2]^{+}$.[5] The microanalytical data of the oxidised species (Experimental section) match well with the dimeric form, **1G** (Scheme 2). The isolated diamagnetic complex **1G** exhibits 1 : 4 conductivity in acetonitrile solvent (Λ_M/Ω^{-1} cm^2 mol^{-1}, 420).

The ^{1}H NMR spectra of the complexes **1**–**5** were recorded in $CDCl_3$ solvent and the spectrum of **2** is shown in Fig. 1(a). The presence of the unsymmetric salicylate group in **1**–**5** makes all the five aromatic rings non-equivalent, the complexes **1** and **2**–**5** thus display twentytwo and twenty non-equivalent aromatic protons (Fig. 1a) respectively.[5] The partial overlapping of the signals makes the assignment of the individual signals difficult, however a careful examination of the spectra clearly indicates the presence of the estimated number of singlet, doublets and triplets as well as the isomeric purity of the products. The complexes **2** and **4** display two closely spaced Me signals each having 1 : 1 intensity ratio in the upfield region (δ 2.143 and 2.131 for **2** and 2.232 and 2.221 for **4**). The isomer **B** should exhibit one Me signal, on the other hand all other isomers (**A**, **C** and **D**) should display two methyl signals having equal intensity. The observed closely spaced two methyl signals presumably provides indirect support in favour of the isomeric structure **A** as this is the only form where both the methyl groups are in the best possible symmetric environment [both are *cis* to pyridine nitrogens (N_p) and *trans* to oxygens (phenolato or carboxylato)].[6]

The ^{1}H NMR spectrum of **1G** in $CDCl_3$ displays signals corresponding to half of the molecule (**1G**) as each half is equivalent due to the localised symmetry (Fig. 1b). The coupling pattern of the resonances particularly in the upfield part of the aromatic region of **1** differs from that of the dimeric complex **1G**. This is due to the fact that the salicylate function in the starting monomeric complexes (**1**–**5**) exists as a four spin system while the same in the oxidised dimeric complex **1G** corresponds to a three spin system.

The formation of **1** and **1G** has been confirmed by electrospray mass spectra (ESI supplementary material). Maximum molecular ion peaks, at *m*/*z* 604.4 (formula weight, 603.60) and 1206.02 (formula weight, 1205.19) are exhibited for **1** and **1G** respectively.

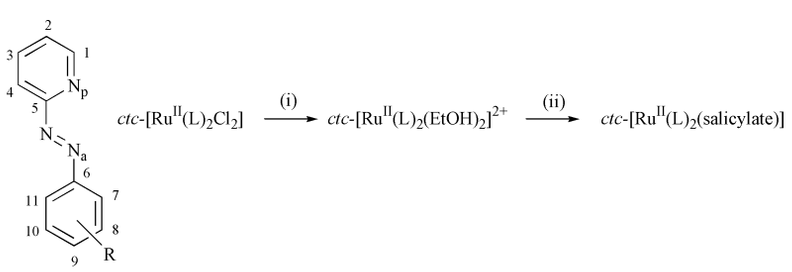

R		
H	L^1	**1**
8-Me	L^2	**2**
8-Cl	L^3	**3**
9-Me	L^4	**4**
9-Cl	L^5	**5**

Scheme 1 (i) Dry EtOH, $AgNO_3$, Δ; (ii) $HO^1C_6H_4C(=O)O^2H$, NaOH, Δ.

Table 1 Electrochemical data in acetonitrile at 298 K [a]

	$[E^\circ_{298}$/V (ΔE_p/mV)]								
			Salicylate based			L based			
Compound	Ru^{III}–Ru^{II} Couple I	n [b]	Couple II	Couple III	Ru^{IV}–Ru^{III} Couple IV	Couple V	Couple VI	Couple VII	Couple VIII
1	0.70(90)	0.96	1.03(100)	1.55(110)	1.97(110)	−0.60(70)	−1.15(80)	−1.93(100)	−2.33(120)
2	0.67(100)	0.95	1.05(100)	1.54(120)	1.94(120)	−0.66(80)	−1.22(80)	−1.99(90)	−2.40(110)
3	0.72(100)	1.05	1.05(80)	1.56(100)	2.00(100)	−0.56(70)	−1.10(80)	−1.80(100)	−1.89(120)
4	0.65(80)	1.07	0.98(100)	1.50(100)	1.89(100)	−0.72(80)	−1.27(80)	−2.09(90)	−2.44(110)
5	0.76(80)	1.05	1.10(80)	1.58(90)	2.09(100)	−0.52(70)	−1.02(80)	−1.71(90)	−1.83(120)

[a] Solvent, acetonitrile; supporting electrolyte, $[NEt_4][ClO_4]$ (concentration $\approx 10^{-1}$ mol dm^{-3}); reference electrode, SCE; solute concentration, $\approx 10^{-3}$ mol dm^{-3}; working electrode, platinum wire. Cyclic voltammetric data: scan rate, 50 mV s^{-1}; $E^\circ_{298} = 0.5\,(E_{pa} + E_{pc})$ where E_{pa} and E_{pc} are the anodic and cathodic peak potentials, respectively. [b] $n = Q/Q'$, where Q' is the calculated coulomb count for 1e$^-$ transfer and Q is the coulomb count found after exhaustive electrolysis of a $\approx 10^{-2}$ mol dm^{-3} solutions of the complexes.

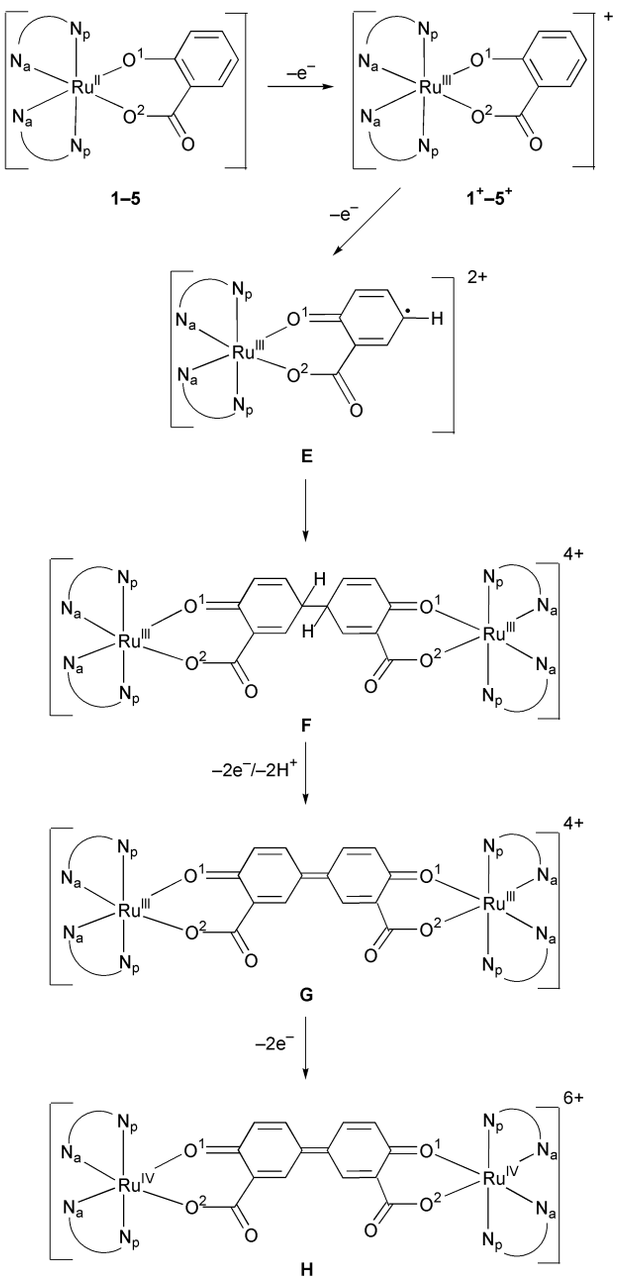

Scheme 2

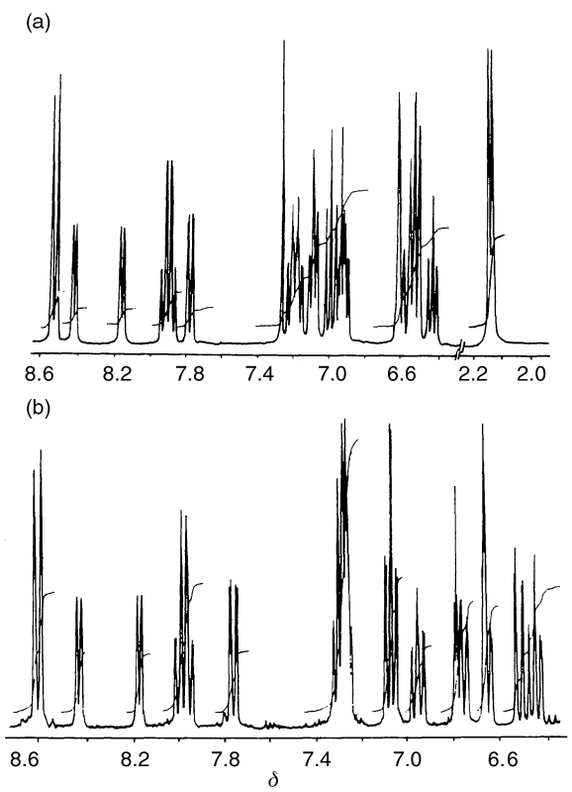

Fig. 1 ^{1}H NMR spectra of (a) $[Ru^{II}(L^2)_2(salicylate)]$ **2** and (b) $[(L^1)_2Ru^{III}\{^-O_2C(O)C_6H_3{=}C_6H_3(O)CO_2^-\}Ru^{III}(L^1)_2][ClO_4]_4\cdot 2H_2O$ **1G** in $CDCl_3$.

Electron-transfer properties

Electron-transfer properties of the complexes **1**–**5** have been studied in acetonitrile solvent using a platinum working electrode. Representative voltammograms are shown in Fig. 2 and the data are listed in Table 1.

The complexes display one quasi-reversible oxidative response in the range 0.65–0.76 V which is assigned to be Ru(III)–Ru(II) couple (I, Fig. 2). The one-electron nature of the couple is confirmed by constant potential coulometry (Table 1). The presence of trivalent ruthenium in the oxidised solution is confirmed by the characteristic rhombic EPR spectra of the ruthenium(III) species in a distorted octahedral arrangement (see later). The potential of couple I varies systematically depending on the electronic nature and location of the 'R' groups present in the framework of L. Coulometric oxidations of the blue-violet starting ruthenium(II) complexes (**1**–**5**) in acetonitrile solvent at a potential ≈100 mV greater than that of the corresponding E_{pa}(couple I) result in a violet oxidised solution. The oxidised complexes ($\mathbf{1}^+$–$\mathbf{5}^+$) show voltammograms which are superimposable on those of the parent bivalent species, implying the stereoretentive nature of the oxidation process. Coulometric reductions of the oxidised violet ruthenium(III) complexes at a potential less than that of the corresponding E_{pc} of couple I produce the parent blue-

Table 2 EPR g values[a] of coulometrically[b] generated trivalent ruthenium(III) species, distortion parameters[c] and NIR transitions[d]

Compound	g_x	g_y	g_z	k	Δ/λ	V/λ	ν_1/λ	ν_2/λ	ν_2/λ_{obs}
$\mathbf{1}^+$	−2.378	−2.105	1.839	0.645	5.072	−3.696	3.375	7.135	7.715
$\mathbf{2}^+$	−2.382	−2.115	1.840	0.661	5.046	−3.552	3.417	7.039	7.756
$\mathbf{3}^+$	−2.389	−2.111	1.840	0.666	5.108	−3.730	3.393	7.187	6.721
$\mathbf{4}^+$	−2.388	−2.109	1.832	0.652	4.956	−3.579	3.321	6.966	7.522
$\mathbf{5}^+$	−2.385	−2.119	1.835	0.661	4.939	−3.401	3.386	6.862	7.589

[a] Measurements were made in dichloromethane at 77 K. [b] Solvent, dichloromethane; supporting electrolyte, $[NEt_4][ClO_4]$ (concentration $\approx 10^{-1}$ mol dm^{-3}); reference electrode, SCE; solute concentration, $\approx 10^{-3}$ mol dm^{-3}; working electrode, platinum wire gauze. [c] Symbols have the same meaning as in the text. [d] In dichloromethane.

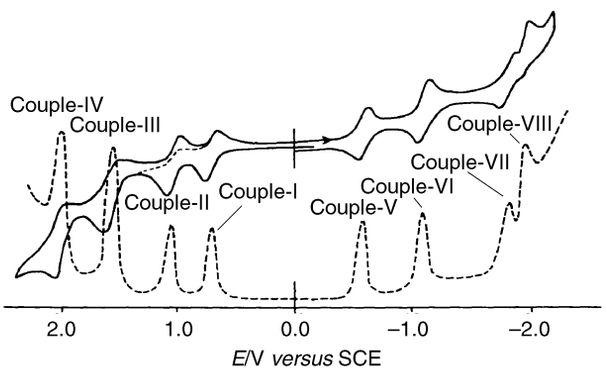

Fig. 2 Cyclic voltammograms and differential pulse voltammograms of the complex $[Ru^{II}(L^3)_2(salicylate)]$ **3** in acetonitrile at 298 K. The dashed line indicates the irreversible nature of couple II.

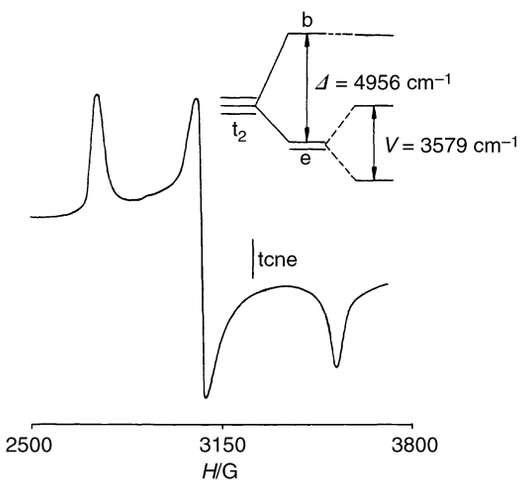

Fig. 3 X-Band EPR spectrum and computed t_2 splitting of the coulometrically oxidised complex $[Ru^{III}(L^4)_2(salicylate)]^+$ $\mathbf{4}^+$ in dichloromethane at 77 K.

violet complexes quantitatively, thus implying the reversibility of the process.

The complexes (**1**–**5**) exhibit a second oxidative process near 1.0 V (Fig. 2, couple II; Table 1). The one-electron nature of the couple has been confirmed by comparing its differential pulse voltammogram current height with that of the previous ruthenium(III)–ruthenium(II) couple. The irreversible nature of this process has been confirmed by reversing the scan direction immediately after the couple II response (Fig. 2, dashed line). The observed cathodic part (i_{pc}) of couple II during the first full scan (Fig. 2, solid line) is possibly developed due to contributions from the other two irreversible responses (couples III and IV). Coulometric oxidations of **1**–**5** at a potential greater than the E_{pa} of couple II develop a light pink solution. After the second step the oxidised solution ($\mathbf{1}^{2+}$–$\mathbf{5}^{2+}$) is found to be EPR inactive even at 77 K.

The two-electron nature of the third (couple III, Fig. 2) and fourth (couple IV, Fig. 2) oxidation processes has been established by comparing their differential pulse voltammetric current heights with those of the previous couples (I and II) (Fig. 2). The irreversible nature of this response has been confirmed further by sweeping the scan beyond couple III but without moving up to couple IV. Coulometric oxidations of the complexes at a potential higher than the E_{pa} of couple III generate a red solution ($\mathbf{1}^{3+}$–$\mathbf{5}^{3+}$) which is also EPR silent at 77 K. Coulometric oxidations of the complexes at a potential greater than the E_{pa} of couple IV provide a very small coulomb count, implying the unstable nature of the oxidised species ($\mathbf{1}^{4+}$–$\mathbf{5}^{4+}$) even on the coulometric timescale.

The complexes display four successive one-electron reductions at negative side potentials with respect to the SCE (couples V–VIII). The one-electron nature of the couples has been identified by comparison with the ruthenium(III)–ruthenium(II) couple (I) with the help of the cyclic voltammetric as well as differential pulse voltammetric current height. The ligand L is known to act as a potential electron-transfer centre and each can accept two electrons in the electrochemically accessible LUMO which is predominantly azo in character.[7] As two electroactive azo groups are present around the ruthenium ion, four successive one electron reductions are expected for each case and in practice all the responses have been nicely observed experimentally (Fig. 2, Table 1).

The coulometrically produced reduced light red solution of $\mathbf{1}^-$–$\mathbf{5}^-$ [obtained by reducing the complexes **1**–**5** at a potential 100 mV more negative than the corresponding E_{pc} of couple V (Fig. 2)] have been found to be unstable. However, the EPR spectrum of the reduced complex $\mathbf{4}^-$ has been recorded by performing the electrolysis at 258 K [observed coulomb count corresponds to one-electron transfer ($n = 1.11$)] and quickly freezing the electrolysed solution at 77 K (liquid nitrogen) (see below).

EPR spectra of the oxidised ($\mathbf{1}^+$–$\mathbf{5}^+$) and reduced ($\mathbf{4}^-$) complexes

The coulometrically oxidised complexes ($\mathbf{1}^+$–$\mathbf{5}^+$ at 258 K) exhibit rhombic EPR spectra (Fig. 3, Table 2) in dichloromethane at 77 K which suggests the correspondence of couple I with the ruthenium(III)–ruthenium(II) process as opposed to ligand based oxidation like the ruthenium–dioxolene system.[8]

The EPR spectra of the oxidised complexes have been analysed in terms of g-tensor theory of low-spin d^5 ions.[9] The axial (Δ) and rhombic (V) distortions (Table 2) combined with spin–orbit coupling [λ for Ru^{III} is 1000 cm^{-1} [10]] transform the t_2 shell into three Kramers doublets. The ligand field transitions ν_1 and ν_2 among them are predicted to lie in the ranges 3321–3417 and 6862–7187 cm^{-1} respectively (Table 2). A relatively weak transition is indeed observed close to the predicted range 6721–7756 cm^{-1} and is assigned to be the ν_2 transition (Table 2). The ν_1 transition lies outside the range of our instrument. The computed distortion parameters (Δ and V, Table 2) indicate the presence of a high degree of rhombicity in the complexes.[11]

The first step reduced complex $\mathbf{4}^-$ in dichloromethane shows an intense and sharp EPR signal at 77 K with a 'g' value at 2.003, implying that the unpaired electron in the reduced product is localised in the orbital which has predominantly

Table 3 Electronic spectral data for the complexes $[Ru(L)_2(salicylate)]$ **1**–**5** and their stepwise electrochemically oxidised products in acetonitrile

Compound	UV/vis λ/nm(ε/dm^3 mol^{-1} cm^{-1})
1	597(10200), 509(3900), 326(24650), 224(47600)
1$^+$	560, 460, 365, 316
1F	549, 452, 358, 309, 282
1G	505, 470, 361, 300, 277
2	598(9500), 507(3560), 328(23460), 218(53430)
2$^+$	562, 455, 378, 322
2F	542, 510, 358, 312, 287
2G	503, 466, 372, 310, 280
3	600(8900), 499(3360), 315(24500), 200(66000)
3$^+$	571, 460, 370, 314
3F	549, 455, 370, 302, 285
3G	510, 478, 351, 314, 283
4	599(10470), 500(4190), 335(23660), 218(50920)
4$^+$	581, 465, 370, 335
4F	548, 455, 380, 312, 289
4G	504, 465, 382, 312, 282
5	602(9370), 500(3700), 331(25000), 223(43640)
5$^+$	575, 465, 370, 331
5F	552, 445, 365, 334, 305
5G	505, 475, 376, 290, 280

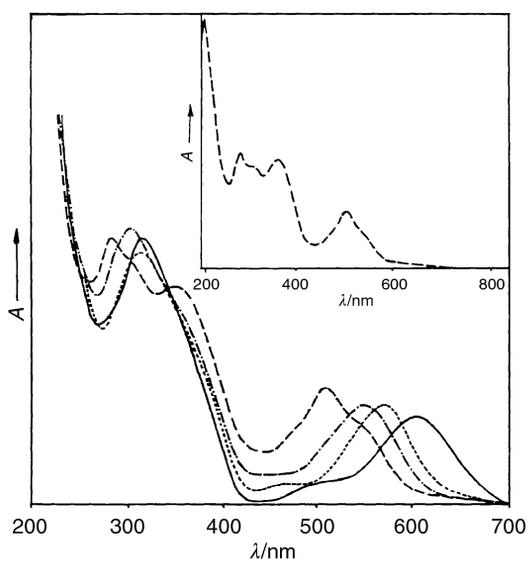

Fig. 4 UV-visible spectra of the complex $[Ru^{II}(L^3)_2(salicylate)]$ **3** (—) and its stepwise electrochemically oxidised products in acetonitrile at 298 K: (·····) **3**$^+$, (-·-·-) **3F**, (---) **3G**. The inset shows the electronic spectrum of the chemically isolated complex, $[(L^1)_2Ru^{III}\{^-O_2C(O)\text{-}C_6H_3\text{=}C_6H_3(O)CO_2^-\}Ru^{III}(L^1)_2][ClO_4]_4\cdot 2H_2O$ **1G**.

ligand character.[12] This supports the successive addition of electrons to the azo functions as considered above. Coulometric reductions of the other couples (VI–VIII) (Fig. 2) generated the unstable reduced species even at 258 K.

Electronic spectra

The solution electronic spectra of the complex **3** and its oxidation products are displayed in Fig. 4 and the data are shown in Table 3. The spectral profiles are similar for all the complexes. In the visible region the complexes exhibit one strong band near 600 nm followed by a shoulder at a higher energy region near 500 nm. The band profiles are similar to those of other reported complexes having the *tc*-$Ru^{II}(L)_2$ moiety, therefore the observed bands are believed primarily to be originating from the $d\pi(Ru^{II}) \longrightarrow L(\pi^*)$ MLCT transitions, where $L(\pi^*)$ is dominated by the LUMO of the azoimine chromophore.[7] In the UV region the complexes exhibit two strong transitions due to the π–π* and n–π* transitions of the coordinated L.[13]

Electronic spectra of the electrogenerated $\mathbf{1}^+$–$\mathbf{5}^+$ in the visible region display a strong band in the range (560–581 nm) followed by a weak shoulder near 460 nm (Fig. 4, Table 3). The bands are assigned to be the LMCT transitions.[14] Thus on metal oxidation the lowest energy charge-transfer transition has reasonably been blue shifted (Table 3). The band maxima are observed to be dependent on the nature of L present in $\mathbf{1}^+$–$\mathbf{5}^+$ (Table 3). The intra ligand π–π* and n–π* transitions have appeared in the UV region as expected (Table 3).

The second- ($\mathbf{1}^{2+}$–$\mathbf{5}^{2+}$) and the third-step oxidised species ($\mathbf{1}^+$–$\mathbf{5}^{3+}$) display the lowest energy LMCT band in the ranges 542–552 and 503–510 nm respectively (Table 3, Fig. 4). Thus the LMCT bands have progressively been blue shifted while moving from $\mathbf{1}^+$–$\mathbf{5}^+ \longrightarrow \mathbf{1}^{2+}$–$\mathbf{5}^{2+} \longrightarrow \mathbf{1}^{3+}$–$\mathbf{5}^{3+}$ due to oxidation of salicylate ligand. In addition in the UV region a greater number of bands have appeared in the cases of $\mathbf{1}^{3+}$–$\mathbf{5}^{3+}$ (Table 3).

Discussion

The ruthenium(III)–ruthenium(II) couple for the complexes **1**–**5** (I, Fig. 2, Table 1) appears in the range 0.65–0.76 V *versus* SCE whereas the same couple for the similar bipyridine complex $[Ru(bpy)_2(salicylate)]$ has been observed at 0.22 V.[3] Therefore, a positive shift of ≈0.4–0.5 V has taken place while moving from the bpy to L^{1-5} environment. This indicates that the stronger π-acidic property of L compared to bpy provides an additional stability to the $t_2(Ru^{II})$ state in **1**–**5**.[15] It may be noted that the ruthenium(II)–dioxolene complexes incorporating L or bpy ancillary ligands, $[Ru^{II}(L \text{ or } bpy)_2(dioxolene)]$, display oxidation of the dioxolene moiety prior to electron transfer at the metal centre.[16]

The difference in potential between the two successive observed couples (II, I, Fig. 2) is approximately 0.3 V. Since the separation between the two consecutive metal based processes $[Ru^{IV}/Ru^{III}\text{–}Ru^{III}/Ru^{II}]$ is known to lie in the range of 1.3–1.5 V,[17] the origin of the second couple (II, Fig. 2) as the next metal based process, ruthenium(III)–ruthenium(IV) oxidation, appears to be most unlikely. On the other hand in the similar bipyridine complex $[Ru^{II}(bpy)_2(salicylate)]$ the salicylate ligand itself takes part in an one-electron oxidation to the semiquinone radical form immediately after the metal oxidation (Ru^{II}–Ru^{III}) process.[3] Thus, by comparison with the bpy system, we ascribe couple II for the present system (**1**–**5**) to oxidation of the coordinated salicylate to semiquinone cation radical, structure **E** in Scheme 2.

In the case of the bipyridine analogue $[Ru^{III}(bpy)(salicylate)]^{2+}$ the semiquinone salicylate cation radical form (**E**) can afford to lose one more electron from the salicylate unit, generating a reactive cationic species which then undergoes hydroxylation at the cationic centre of the salicylate moiety.[3] However, in the present case the electrogenerated cation radical (structure **E**) is found to be reactive enough and instead of losing one more electron like the bipyridine complex it follows the natural radical recombination pathway and this leads to the formation of a dimeric complex (structure **F**, Scheme 2). This assumption of dimeric complex (**F**) formation (Scheme 2) through the radical recombination pathway finds appropriate justification based on the redox steps which are observed subsequently (see later).

The difference in behaviour of the coordinated salicylate semiquinone radical moiety (**E**) depending on the nature of the ancillary functions (bpy and L) may be rationalised based on their inherent difference in π-acidic property. Here the cationic radical is stabilised by L and that is why it is difficult to oxidise again and instead dimerises. The irreversible nature of couple II (Fig. 2, dashed line) also indicates that the electrochemically generated semiquinone radical (**E**) dimerises rapidly, therefore on scan reversal the reduced form of **E** does not reappear. The two-electron nature of couple III (Fig. 2, Table 1) provides

strong support in favour of our earlier consideration of dimerisation (**F**) of the semiquinone radical (**E**). We believe that this couple involves a simultaneous $2e^-/2H^+$-transfer process associated with the bridging part of the dimeric species **F** (Scheme 2) which eventually provides additional conjugation to the bridging unit (structure **G**).[5] The irreversible nature of couple III implies that the proton loss takes place because electrochemical oxidation of **F** ⟶ **G** cannot occur during electrochemical reduction of **G**, particularly in the non-protic acetonitrile solvent. The diamagnetic nature of the oxidised $\mathbf{1}^{2+}$–$\mathbf{5}^{2+}$ species indicates that the two ruthenium(III) (t_{2g}^5, $S = \frac{1}{2}$) centres in **F** are antiferromagnetically coupled.[8,18]

The electronic spectra of the third-step oxidised species ($\mathbf{1}^{3+}$–$\mathbf{5}^{3+}$) display the lowest energy LMCT band near 500 nm which has considerably been blue shifted as compared to the previous step oxidised species, $\mathbf{1}^{2+}$–$\mathbf{5}^{2+}$ (550 nm) (Table 3, Fig. 4). Moreover, the UV region of $\mathbf{1}^{3+}$–$\mathbf{5}^{3+}$ has become more prominent (Fig. 4) due to the introduction of additional conjugation in the structure **G**. Thus spectroelectrochemical studies can provide suitable justifications in favour of the conversion of **F** ⟶ **G** on oxidation.

The assignment of the observed fourth-step, simultaneous two-electron oxidation process (couple IV, Fig. 2) corresponding to the ruthenium(III)–ruthenium(IV) oxidation process (structure **H**, Scheme 2) is made based on the fact that the organic fragments associated with the complex moiety (**G**) are in their possible oxidised form.[19] The potential difference (ΔE) between the two successive oxidation processes of the ruthenium centre ($Ru^{II/III}$–$Ru^{III/IV}$) is observed to be ≈1.3 V (Table 2) which matches well with earlier reported values (≈1.3–1.5 V).[17]

The UV-visible spectrum of the chemically oxidised species is identical with that of the red solution obtained separately from the third-step (couple III) electrochemical oxidation (Fig. 4, inset). Hence, this confirms that the HNO_3 oxidation product essentially represents the dimeric form '**G**' as shown in Scheme 2. The isolated oxidised complex (**1G**) exhibits a ruthenium(III)–ruthenium(IV) couple at the same potential (2.0 V *versus* SCE) as observed in the case of the corresponding red solution obtained *via* the third-step electrochemical oxidation.

Although we were unable to grow suitable single crystals for X-ray characterisation, the mass, microanalytical, conductivity, ^{1}H NMR and spectroelectrochemical studies collectively establish the composition, stereochemistry and the reactivity pattern of the complexes.

Conclusion

We have observed that the reactivity pattern of ruthenium salicylates incorporating strongly π-acidic azopyridine ancillary ligands (L) is markedly different from that of the bipyridine analogue. The reactivity of the electrogenerated coordinated semiquinone salicylate cation radical (**E**) is primarily guided by the electronic aspects of the ancillary functions (L and bpy). Hence, in the presence of bipyridine the salicylate semiquinone cationic radical (**E**) undergoes hydroxylation *via* the formation of a cationic species. On the contrary the presence of the stronger π-acidic 'L' facilitates the radical recombination pathway leading to dimerisation followed by successive electron transfer and proton transfer at the metal and the bridging ligand sites. To the best of our knowledge the present work demonstrates for the first time the electro-non-innocent behaviour of the coordinated salicylate function leading to the formation of a new class of coordinated semiquinone salicylate based bridging ligand. Further work is in progress in order to scrutinise the reactivity features of ruthenium salicylates in combination with other ancillary ligands having different electronic natures.

Experimental

Materials

Commercial ruthenium trichloride (S.D. Fine Chemicals, Bombay, India) was converted into $RuCl_3 \cdot 3H_2O$ by repeated evaporation to dryness with concentrated hydrochloric acid. The starting complexes *ctc*-$Ru(L)_2Cl_2$ were prepared according to the reported procedure.[20] Salicylic acid was purchased from Aldrich, USA. Other chemicals and solvents were reagent grade used as received. Silica gel (60–120 mesh) and alumina (neutral) were used for chromatographic purifications. For spectroscopic and electrochemical studies HPLC grade solvents were used. Commercial tetraethylammonium bromide was converted into pure tetraethylammonium perchlorate by following an available procedure.[21]

Physical measurements

UV-visible spectra were recorded by using a Shimadzu-2100 spectrophotometer, FT-IR spectra on a Nicolet spectrophotometer with samples prepared as KBr pellets. Solution electrical conductivity was checked using a Systronic 305 conductivity bridge. Magnetic susceptibility was measured with a PAR vibrating sample magnetometer. Cyclic voltammetric, differential pulse voltammetric and coulometric measurements were carried out using a PAR model 273A electrochemistry system. Platinum wire working and auxiliary electrodes and an aqueous saturated calomel reference electrode (SCE) were used in a three electrode configuration. The supporting electrolyte was $[NEt_4][ClO_4]$ and the solute concentration was $\approx 10^{-3}$ mol dm^{-3}. The half-wave potential E°_{298} was set equal to 0.5 ($E_{pa} + E_{pc}$), where E_{pa} and E_{pc} are the anodic and cathodic cyclic voltammetric peak potentials respectively. A platinum wire-gauze working electrode was used in coulometric experiments. All experiments were carried out under a dinitrogen atmosphere and were uncorrected for junction potentials. The EPR measurements were made with a Varian model 109C E-line X-band spectrometer fitted with a quartz Dewar for measurements at 77 K (liquid nitrogen). The spectra were calibrated by using tetracyanoethylene (tcne, $g = 2.0023$). The electrospray mass spectra were recorded on a Micromass Quattro II triple quadrupole mass spectrometer. The elemental analyses were carried out with a Carlo Erba (Italy) elemental analyser.

Preparation of complexes

The complexes $[Ru^{II}(L^{1-5})_2(salicylate)]$ **1**–**5** were synthesized from the corresponding starting $[Ru^{II}(L^{1-5})_2(EtOH)_2]^{2+}$ species by following a general procedure. Yields vary in the range 70–75%. Details are given for one representative complex (**1**).

$[Ru(L^1)_2(salicylate)]$ 1. Initially a solution of $[Ru^{II}(L^1)_2(EtOH)_2]^{2+}$ was prepared by stirring under reflux condition a mixture of $Ru(L^1)_2Cl_2$ (100 mg, 0.186 mmol) and $AgNO_3$ (79 mg, 0.465 mmol) in dry ethanol (20 cm^3) for 1 h and removing the AgCl precipitate. To the filtrate were added an excess of salicylic acid (65 mg, 0.471 mmol) and NaOH (38 mg, 0.95 mmol) and the solution was heated to reflux for 12 h under a dinitrogen atmosphere, during which time it changed from purple to blue-violet. The solvent was then removed under reduced pressure and the solid mass thus obtained purified by using a alumina (neutral) column. A blue-violet band corresponding to **1** was eluted with acetonitrile. On evaporation the solid complex was obtained in 72% yield (81 mg). Finally the product was recrystallised from 1 : 4 v/v dichloromethane–light petroleum (bp 40–60 °C).

Calc. for **1**: C, 57.71; H, 3.67; N, 13.92. Found: C, 57.62; H, 3.48; N, 13.75. Calc. for **2**: C, 58.95; H, 4.15; N, 13.30. Found: C, 58. 61; H, 4.40; N, 13.49. Calc. for **3**: C, 51.79; H, 2.99; N,

12.50. Found: C, 52.11; H, 2.88; N, 12.76. Calc. for **4**: C, 58.95; H, 4.15; N, 13.30. Found: C, 58.72; H, 4.44; N, 13.67. Calc. for **5**: C, 51.79; H, 2.99; N, 12.50. Found: C, 52.17; H, 3.26; N, 12.82%.

The complex **1G** was prepared from **1** by using concentrated HNO_3 as follows. The starting complex $[Ru(L^1)_2(salicylate)]$ (100 mg) was taken in distilled water (20 cm^3) and heated to reflux for 15 min. Concentrated HNO_3 (0.5 cm^3) was added dropwise and the mixture heated to reflux for another 1 h, during which time it changed from blue-violet to red. The volume was then reduced to 5 cm^3 on a water bath and saturated aqueous $NaClO_4$ solution added. The mixture was kept in a refrigerator overnight. The dark crystalline solid deposited was collected by filtration, washed with cold water and dried *in vacuo* over P_4O_{10}. The solid mass was purified by using a silica gel column. A red band corresponding to **1G** was eluted with dichloromethane–methanol (10 : 0.5). On removal of solvent the pure solid complex was obtained. Yield 176 mg (65%). The complex was recrystallised from acetonitrile–benzene (1 : 5 v/v). Calc. for $C_{58}H_{46}Cl_4N_{12}O_{24}Ru_2$ **1G**: C, 42.50; H, 2.83; N, 10.25. Found: C, 42.81; H, 3.02, N, 10.70%.

Acknowledgements

Financial supports received from the Department of Science and Technology, New Delhi and Council of Scientific and Industrial Research, New Delhi, India, are gratefully acknowledged. Special acknowledgement is made to Regional Sophisticated Instrumental Centre (RSIC), Indian Institute of Technology, Bombay for providing the NMR and EPR facilities. The referees comments at the revision stage were very helpful.

References

1 B. Kalyanaraman, S. Ramanujam, R. J. Singh, J. Joseph and J. B. Feix, *J. Am. Chem. Soc.*, 1993, **115**, 4007; R. A. Floyd, J. J. Watson and P. K. Wong, *J. Biochem. Biophys. Methods*, 1984, **10**, 221; R. A. Floyd, R. Henderson, J. J. Watson and P. K. Wong, *J. Free Radicals Biol. Med.*, 1986, **2**, 13; K. O. Hiller and R. L. Wilson, *Biochem. Pharmacol.*, 1983, **32**, 2109; M. Grootveld and B. Halliwell, *Biochem. J.*, 1986, **237**, 499; Z. Maskos, J. D. Rush and W. H. Koopenol, *Free Radicals Biol. Med.*, 1990, **8**, 153.

2 A. Pramanik, N. Bag and A. Chakravorty, *J. Chem. Soc.*, *Dalton Trans.*, 1992, 97.

3 V. R. L. Constantino, H. E. Toma, L. F. C. deOliveira, F. N. Rein, R. C. Rocha and D. deOliveira Silva, *J. Chem. Soc.*, *Dalton Trans.*, 1999, 1735.

4 B. K. Santra and G. K. Lahiri, *J. Chem. Soc.*, *Dalton Trans.*, 1997, 129; B. K. Santra, G. A. Thakur, P. Ghosh, A. Pramanik and G. K. Lahiri, *Inorg. Chem.*, 1996, **35**, 3050; P. S. Rao, G. A. Thakur and G. K. Lahiri, *Indian J. Chem.*, *Sect. A*, 1996, **35**, 946 and references therein.

5 G. K. Lahiri, S. Bhattacharya, S. Goswami and A. Chakravorty, *J. Chem. Soc.*, *Dalton Trans.*, 1990, 561; T. Mizoguchi and R. N. Adams, *J. Am. Chem. Soc.*, 1962, **84**, 2058; Z. Galus and R. N. Adams, *J. Am. Chem. Soc.*, 1962, **84**, 2061; R. N. Adams, *Electrochemistry at Solid Electrodes*, Marcel Dekker, New York, 1969.

6 S. Goswami, R. N. Mukherjee and A. Chakravorty, *Inorg. Chem.*, 1983, **22**, 2825.

7 S. Goswami, A. R. Chakravarty and A. Chakravorty, *Inorg. Chem.*, 1981, **20**, 2246; R. A. Krause and K. Krause, *Inorg. Chem.*, 1982, **21**, 1714.

8 B. Mondal, S. Chakraborty, P. Munshi, M. G. Walawalkar and G. K. Lahiri, *J. Chem. Soc.*, *Dalton Trans.*, 2000, 2327; S. Chakraborty, M. G. Walawalkar and G. K. Lahiri, *J. Chem. Soc.*, *Dalton Trans.*, 2000, 2875; B. M. Holligan, J. C. Jeffery, M. K. Norgett, E. Schatz and M. D. Ward, *J. Chem. Soc.*, *Dalton Trans.*, 1992, 3345.

9 B. K. Santra, M. Menon, C. K. Pal and G. K. Lahiri, *J. Chem. Soc.*, *Dalton Trans.*, 1997, 1387; P. Munshi, R. Samanta and G. K. Lahiri, *J. Organomet. Chem.*, 1999, **586** 176; R. Hariram, B. K. Santra and G. K. Lahiri, *J. Organomet. Chem.*, 1997, **540**, 155; G. K. Lahiri, S. Bhattacharya, B. K. Ghosh and A. Chakravorty, *Inorg. Chem.*, 1987, **26**, 4324; C. Daul and A. Goursot, *Inorg. Chem.*, 1985, **24**, 3554; R. E. Desimone and R. S. Drago, *J. Am. Chem. Soc.*, 1970, **92**, 2343.

10 E. M. Kober and T. J. Meyer, *Inorg. Chem.*, 1983, **22**, 1614.

11 P. Ghosh, A. Pramanik, N. Bag, G. K. Lahiri and A. Chakravorty, *J. Organomet. Chem.*, 1993, **454**, 237.

12 M. D. Ward, *Inorg. Chem.*, 1996, **35**, 1712; R. Samanta, P. Munshi, B. K. Santra and G. K. Lahiri, *Polyhedron*, 1999, **18**, 995; A. K. Deb and S. Goswami, *J. Chem. Soc.*, *Dalton Trans.*, 1989, 1635.

13 B. K. Santra and G. K. Lahiri, *J. Chem. Soc.*, *Dalton Trans.*, 1998, 139; A. Bharath, B. K. Santra, P. Munshi and G. K. Lahiri, *J. Chem. Soc.*, *Dalton Trans.*, 1998, 2643.

14 S. Kulkarni, B. K. Santra, P. Munshi and G. K. Lahiri, *Polyhedron*, 1998, **17**, 4365.

15 B. Mondal, M. G. Walawalkar and G. K. Lahiri, *J. Chem. Soc.*, *Dalton Trans.*, 2000, 4209; J. L. Robertson, A. Kadziola, R. A. Krause and S. Larsen, *Inorg. Chem.*, 1989, **28**, 2097.

16 C. G. Pierpont and C. W. Lange, *Prog. Inorg. Chem.*, 1994, **41**, 331; R. A. Metcalfe and A. B. P. Lever, *Inorg. Chem.*, 1997, **36**, 4762; F. Hartl, T. L. Snoeck, D. J. Stufkens and A. B. P. Lever, *Inorg. Chem.*, 1995, **34**, 3887; H. Masui, A. B. P. Lever and E. S. Dodsworth, *Inorg. Chem.*, 1993, **32**, 258; H. Masui, A. B. P. Lever and P. R. Auburn, *Inorg. Chem.*, 1991, **30**, 2402; A. M. Barthram, R. L. Cleary, R. Kowallick and M. D. Ward, *Chem. Commun.*, 1998, 2695; N. Bag, A Pramanik, G. K. Lahiri and A. Chakravorty, *Inorg. Chem.*, 1992, **31**, 40; N. Bag, G. K. Lahiri, P. Basu and A. Chakravorty, *J. Chem. Soc.*, *Dalton Trans.*, 1992, 113.

17 N. Bag, G. K. Lahiri, S. Bhattacharya, L. R. Falvello and A. Chakravorty, *Inorg. Chem.*, 1988, **27**, 4396; G. K. Lahiri, S. Bhattacharya, M. Mukherjee, A. K. Mukherjee and A. Chakravorty, *Inorg. Chem.*, 1987, **26**, 3359.

18 C. Trindle and S. N. Dutta, *Int. J. Quantum Chem.*, 1996, **57**, 781.

19 E. Ishow, A. Gourdon, J. P. Launay, C. Chiorboli and F. Scandola, *Inorg. Chem.*, 1999, **38**, 1504.

20 P. Munshi, R. Samanta and G. K. Lahiri, *Polyhedron*, 1998, **17**, 1913.

21 D. S. Sawyer, A. Sobkowiak and J. L. Roberts, Jr., *Experimental Electrochemistry for Chemists*, Wiley, New York, 1995.